Nonlinear Optics in Relativistic Plasmas

D. Umstadter, S.-Y. Chen, G.S. Sarkisov, A. Maksimchuk, and R. Wagner

Center for Ultrafast Optical Science[1]
University of Michigan
Ann Arbor, MI 48109-2099

Abstract. We discuss various nonlinear optical processes that occur as an intense laser propagates through a relativistic plasma. These include the experimental observations of electron acceleration driven by laser-wakefield generation, relativistic self-focusing, waveguide formation and laser self-channeling.

INTRODUCTION

Due to recent advances in laser technology [1], it is now possible to generate the highest electromagnetic and electrostatic fields ever produced in the laboratory [2]. The interactions of such high-intensity and ultrashort-duration laser pulses with plasmas permits for the first time the study of optics in relativistic plasmas. Technological applications include advanced fusion energy, x-ray lasers, and table-top ultrahigh-gradient electron accelerators.

We have recently demonstrated that by simply focusing a table-top size, high-power (terawatt) laser into a gas, a beam of relativistic electrons is produced. It is accelerated up to an energy of 40 MeV by a laser-wakefield plasma wave in a distance less than one millimeter. The accelerated electron beam appeared to be naturally-collimated with a low-divergence angle and had over a nanocoulomb of charge in a 1-picosecond duration pulse. These characteristics are comparable to those of state-of-the-art radio-frequency linacs, but the acceleration length is ten-thousand times shorter. This enormous field gradient (2 GeV/cm)—which is the highest terrestrial electrostatic field ever recorded—would be of limited use if its length were limited by laser diffraction. Fortunately, we also recently showed that—above a certain laser power—the

plasma acts like a lens, which guides the laser beam by a process called relativistic self-focusing. The relativistically self-guided channel was found to extend the laser propagation distance to many Rayleigh lengths, decrease the electron beam divergence and increase the electron energy. Where the laser was guided, an on-axis density depression was also observed to form, created by electron cavitation due to laser pressure followed by Coulomb explosion of the ions. Another intense laser pulse that was delayed in time with respect to the first was shown to propagate down the channel. Finally, we discuss optical injection of electrons into wakefield plasma waves.

When an intense laser enters a region of gaseous-density atoms, the atomic electrons feel the enormous laser electromagnetic field, and begin to oscillate at the laser frequency $(\omega = 2\pi c/\lambda = ck)$. The oscillations can become so large that the electrons become stripped from the atoms, or ionized. At high laser intensity (I), the free electrons begin to move at close to the speed of light (c), and thus their mass m_e changes significantly compared to their rest mass. This large electron oscillation energy corresponds to gigabar laser pressure, displacing the electrons from regions of high laser intensity. Due to their much greater inertia, the ions remain stationary, providing an electrostatic restoring force. These effects cause the plasma electrons to oscillate at the plasma frequency (ω_p) after the laser pulse passes by them, creating alternating regions of net positive and negative charge, where $\omega_p = \sqrt{4\pi e^2 n_e/\gamma m_e}$, n_e is the electron density, e is the electron charge and γ is the relativistic factor associated with the electron motion transverse to the laser propagation. γ depends on the normalized vector potential, a_o, by $\gamma = \sqrt{1 + a_o^2}$, where $a_o = \gamma v_{os}/c = eE/m_o\omega c = 8.5 \times 10^{-10}\lambda[\mu m]I^{1/2}[W/cm^2]$. The resulting electrostatic wakefield plasma wave propagates at a phase velocity nearly equal to the speed of light and thus can continuously accelerate hot electrons [3]. Up to now, most experiments have been done in the self-modulated laser wakefield regime [4–6], where the laser pulse duration is much longer than the plasma period, $\tau >> \tau_p = 2\pi/\omega_p$. In this regime, the forward Raman scattering instability can grow; where an electromagnetic wave $(\omega_o, \mathbf{k}_o)$ decays into a plasma wave $(\omega_p, \mathbf{k}_p)$ and electromagnetic side-bands $(\omega_o \pm \omega_p, \mathbf{k}_o \pm \mathbf{k}_p)$.

Wakefield acceleration, as well as most other applications, depends critically on long-distance propagation of laser pulses at relativistic intensities $(\sim 10^{18}$ W/cm^2 for 1-μm wavelength light). In order to reach such high intensities, laser pulses are usually focused tightly, which, due to diffraction, results in a short interaction length $(\sim$ 1–2 Rayleigh ranges, $Z_R = \pi r_0^2/\lambda)$. Several methods have been proposed to extend the propagation distance of pulses beyond this diffraction limit, as reviewed in [9].

For optical guiding of laser pulses in plasmas, the radial profile of the index of refraction, $n(r)$, must have a maximum on axis, causing the wavefront to curve inward and the laser beam to converge. When this focusing force is strong enough to counteract the diffraction of the beam, the laser pulse can

propagate over a long distance and maintain a small cross section. The index of refraction for a plasma is given by $n(r) = 1 - (\omega_p^2/\omega_0^2) \cdot (n_e(r)/n_{e0}\gamma(r))$, where ω_p is the plasma frequency for electron density n_{e0}, ω_0 is the laser frequency, $n_e(r)$ is the radial distribution of electron density, and $\gamma(r)$ is the relativistic factor associated with the electron motion transverse to the laser propagation. The factor γ depends on the normalized vector potential, a_o, by $\gamma = \sqrt{1 + a_o^2}$, where $a_o = \gamma v_{os}/c = eE/m_o\omega c = 8.5 \times 10^{-10}\lambda[\mu m]I^{1/2}[\text{W/cm}^2]$. It can readily be seen from this that an on-axis maximum of $n(r)$ can be created through modification of the radial profile of γ and/or n_e.

In the former case, $\gamma(0) > \gamma(r)$ can be created by a laser beam with an intensity profile peaked on axis. When a pulse guides itself by this mechanism, it is referred to as relativistic self-guiding, and should occur provided the laser power exceeds a critical power given by $P_c = 17(\omega_0/\omega_p)^2$. A somewhat higher threshold is expected if the ionization defocusing effect is taken into account. In the latter case, $n_e(0) < n_e(r)$ is predicted to occur when the laser's ponderomotive force expels electrons radially from the region of the axis, so called "electron cavitation." Ponderomotive self-channeling [10,11] is expected to enhance the effects of relativistic self-guiding. Self-guiding has previously been observed experimentally [12,30], but electron cavitation has not.

Eventually, after a period of sustained electron expulsion, the ions are predicted to also blow out of the axial region [14] due to Coulomb repulsion, forming a channel [15] that could be used to guide a second laser pulse. A plasma-channel waveguide preformed in this way can guide a relatively high laser intensity ($\geq 10^{17}$ W/cm^2) in a relatively high plasma density ($\geq 10^{19}$cm^{-3}), as compared with waveguides formed by long-duration laser pulses via thermal hydrodynamic expansion followed shock front formation ($\leq 10^{16}$W/cm^2, $\leq 10^{18}$cm^{-3}).

EXPERIMENTS

Experimental Arrangement

In this experiment, we used a Ti:sapphire-Nd:glass laser system based on chirped-pulse-amplification that produces 3 J, 400 fs pulses at 1.053 μm. The 43 mm diameter beam was focused with an f/4 off-axis parabolic mirror to $r_o = 8.5$ μm ($1/e^2$), corresponding to vacuum intensities exceeding 4×10^{18} W/cm^2. This pulse was focused onto a supersonic helium gas jet with a sharp gradient (250 μm) and a long flat-topped interaction region (750 μm). The maximum density varies linearly with backing pressure up to the maximum backing pressure of 1000 PSI, and an underdense plasma at 3.6×10^{19} cm^{-3} is formed by the foot of the laser pulse tunnel-ionizing the gas. This plasma

density corresponds to a critical power of $P_c = 470$ GW. A sharp gradient and long interaction region are found to be essential.

Wakefield Acceleration

Recently, we have shown that an accelerated electron beam appeared to be naturally-collimated with a low-divergence angle (less than ten degrees), and had over 1-nC of charge per bunch [16]. Moreover, as shown in Fig. 1, acceleration occured in this experiment [16] only when the laser power exceeded a certain critical value, P_c, the threshold for relativistic self-focusing.

The total number of accelerated electrons (at all energies) was measured using either a Faraday cup or a plastic scintillator coupled to a photomultiplier tube, and the results were found to be consistent with each other. There is a sharp threshold for electron production at $\sim 1.5P_c$, and the total number of electrons increases exponentially and finally saturates beyond $4P_c$ [16]. At $6P_c$, 6×10^9 accelerated electrons were measured coming out of the plasma in a beam. By using aluminum absorbers, we determined that 50% of the electrons detected have energy greater than 1 MeV (corresponding to 0.5 mJ of energy in the electron beam).

The electron energy spectrum (see Fig. 1) was measured using a 60° sector dipole magnet by imaging a LANEX scintillating screen with a CCD camera. The normalized distribution is found to have a functional form of $\exp(-\alpha\gamma)$ where α is a fitting parameter. In the low power case ($< 6P_c$, no channeling), the normalized distribution follows $\exp(-\gamma)$, and when the laser power
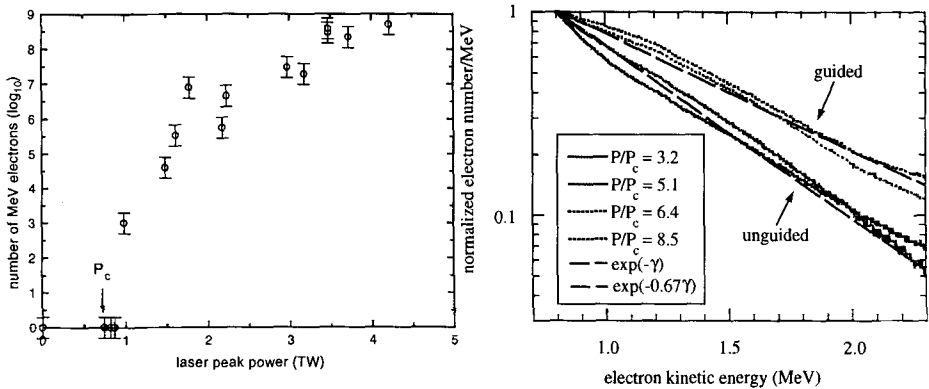
FIGURE 1. The number of relativistic electrons accelerated as a function of incident laser power focused in a gas of helium at atmospheric density. (right) Normalized electron kinetic energy spectrum as a function of laser power at fixed electron density. The upper curves represent the spectra obtained when self-guiding was observed; the lower curves represent unguided spectra.

increases ($> 6P_c$, with channeling), the electron energy distribution discretely jumps to follow $\exp(-0.67\gamma)$. The abrupt change in the electron distribution also occurs if the laser power is held fixed and the density is increased, as it should given the critical power threshold dependence on density. Below 850 PSI (3.1×10^{19} cm^{-3}, no channeling), the electron distribution follows the same trend as the lower power distribution, and above 850 PSI (with channeling) it follows the higher power distribution. For the electron energy distribution greater than 3 MeV, a significantly less steep slope that extends to 20 MeV was measured using aluminum absorbers. Even though the plasma wave amplitude increases as the laser power increases, the distribution only dramatically changes when self-guiding occurs. This indicates that extension in the accelerating length is the primary factor in determining the fitting parameter α.

Measurements of the satellites in the spectrum of the forward scattered light indicated that a self-modulated plasma wave occurred when the laser power exceeded $P_c/2$. Since then, two independent research groups have simultaneously reported direct measurements of the plasma wave amplitude with a Thomson-scattering probe pulse [28,29]. The field gradient was reported [29] to exceed that of a radio-frequency (RF) linac by four orders of magnitude ($E \geq 200$ GV/m). This acceleration gradient corresponds to an energy gain of 1 MeV in a distance of only 10 microns. The plasma wave was observed to exist for a duration of 1.5 ps or 100 plasma oscillations [29]. It was calculated that it damps only because all of the wave energy was converted to the accelerated electrons. Except for the large energy spread and low average power, these parameters compare favorably with medical linacs. In fact, the much smaller source size of a laser wakefield accelerator compared with that of a conventional linac, 10 microns compared with greater than 100 microns, may permit much greater spatial resolution for medical imaging.

Relativistic Self-Guiding

This enormous field gradient would be of limited use if the length over which it could be used to accelerate electrons were just the natural diffraction length of the highly focused laser beam, which is much less than a millimeter. Fortunately, we recently demonstrated that electrons can be accelerated beyond this distance [30]. At high laser power, the index of refraction in a plasma varies with the radius. This is both because the laser intensity varies with radius and the plasma frequency depends on the relativistic mass factor γ. Above the above-mentioned critical laser power P_c, the plasma should act like a positive lens and focus the laser beam, a process called relativistic self-focusing. This is similar to propagating a low power beam over an optical fiber optic cable, except in this case the intense laser makes its own fiber optic.

In order to diagnose the spatial extent of the plasma, a sidescattering imag-

ing system with a spatial resolution of 15 μm was utilized. We were able to resolve the growth of the plasma channel as a function of both laser power and plasma density. Fig. 2 shows the sidescattered intensity distribution as a function of laser power, and the plasma channel clearly extends as the laser power increases. In the lower power cases ($< 2.6P_c$), the channel length is only ~ 125 μm, which is smaller than the confocal parameter ($2Z_R$) of 430 μm. As the laser power increases for a fixed gas density, the channel length first jumps to 250 μm at $3.9P_c$ and then reaches 750 μm at $7.2P_c$. The maximum channel length was observed to be 850 μm at $9.1P_c$. Note this is limited by the interaction length of the gas jet. At $5.5P_c$, the sidescattered image formed has two distinct foci, and when the power exceeds $7.2P_c$, either multiple foci or a channel are observed, depending on shot-to-shot fluctuations and the gas jet position. A similar channel extension occurs if the gas density is varied at fixed laser power. For a 3.9 TW laser pulse, the channel extends to 250 μm at 400 PSI backing pressure (1.4×10^{19} cm^{-3}, $3.2P_c$) and 750 μm at 800 PSI (2.9×10^{19} cm^{-3}, $7.0P_c$). The consistent behavior at specific values of P_c for varying laser power or plasma density indicates that the channeling mechanism is relativistic self-focusing.

The sidescattered light was spectrally analyzed by an imaging spectrometer, and the bulk of the emission comes from incoherent Thomson scattering of the blue-shifted laser pulse. We were unable to obtain any information about the plasma density or temperature from this measurement. The divergence of the laser beam transmitted through the plasma was measured using a diffusing screen and a CCD camera with a 1.053 μm narrow bandpass filter. At all laser powers, the laser expands to twice the vacuum divergence, and we attribute this expansion to ionization defocusing. This is consistent with the strong
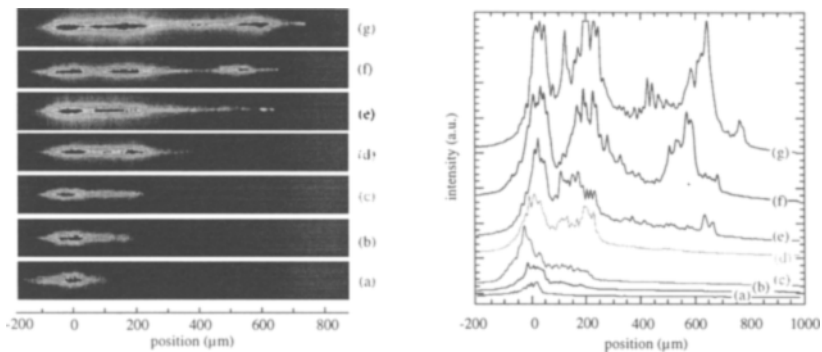
FIGURE 2. On-axis images (left) and corresponding lineouts (right) of sidescattered light at various laser powers and a fixed initial electron density of 3.6×10^{19} cm^{-3}. The various images and lineouts represent laser powers of $P/P_c =$ (a) 1.6, (b) 2.6, (c) 3.9, (d) 5.5, (e) 7.2, (f) 8.4, and (g) 9.1. Note: the curves have been displaced vertically for ease of viewing.

blue-shifting we observe in the scattered spectra. Even though simulations indicate that the laser focuses to ~ 2 μm [19], the complex dynamics that occur as the laser continually focuses and defocuses in the plasma make it impossible to determine the minimum self-focused beam width from the far field divergence angle.

A Maxwellian-like energy distribution has been observed in many previous experiments [20] and simulations [21], however no theoretical justification for it has been found to date. Because the energy distribution is exponential, a temperature in the longitudinal direction can be defined. The temperature of the low energy distribution changes from 500 keV (without guiding) to 750 keV (with guiding). In these plasmas, many different plasma waves can grow from various instabilities and local conditions. The interactions between these waves can lead to stochastic heating of the electron beam, so by extending the plasma length, the various waves will interact longer and heat the beam more. However, the dephasing length, $L_d = \lambda(\omega_o/\omega_p)^3$, which gives the maximum distance over which acceleration can occur (170 μm for our conditions), is significantly shorter than our accelerating length. From this expression, we would think that there would be no noticeable change in the electron spectrum when we extend the plasma length from 250 μm to 750 μm. Recent PIC simulations [21] indicate that this expression is too conservative for these highly nonlinear plasma interactions, and, in fact, the actual dephasing length may be many times longer. Consistent with our experimental results, these simulations indicate that the electron temperature, as well as the maximum energy, increase as the electrons propagate beyond the conventional dephasing length.

The relativistically self-guided channel was found to increase the laser propagation distance by a factor of four (limited thus far only by the length of gas), decrease the electron beam divergence by a factor of two (as shown in Fig. 3), and increase the electron energy.

The electron beam profile was measured using a LANEX scintillating screen imaged by a CCD camera [16]. The LANEX is placed behind an aluminum sheet which blocks the laser light, so only electrons greater than 100 keV can be imaged. Analysis of the electron spectrum indicates that the bulk of the electrons that create an image on the screen are in the 100 keV to 3 MeV range. We have found, using aluminum absorbers, that the electron divergence does not depend on electron energy in this range. At low power ($< 5P_c$), the electron beam has a Gaussian-like profile with a 10° radius at half-maximum (see Fig. 3). As the laser power increases and the plasma channel length increases to ~ 250 μm, a second peak seems to grow out of the low-power profile. Ultimately at the highest laser powers and longest channel lengths, the divergence decreases to 5°, and the profile becomes more Lorentzian-like. The electron beam divergence should decrease as the longitudinal energy of the electrons increases since space charge will be less and the relative transverse momentum decreases due to the longer accelerating length. However, there

should be a minimum divergence due to the space charge effect after the electrons leave the plasma. This effect is significant since the electrons are in the few MeV range (small γ) and the peak current is high (large number of electrons in a short bunch). We have roughly estimated the space charge divergence to be 6° by assuming 10^9 electrons at 1 MeV in a 1 ps bunch (note: $\theta_{hwhm} \propto \sqrt{N/\tau_e(\beta\gamma)^3}$, where N is the number of electrons, τ_e is the electron bunch duration, and $\beta\gamma$ is the normalized momentum of the electrons) [22]. The electron beam emittance can be found from the measured divergence angle and the radius of the plasma channel, and in the best case (5° half-angle and 5 μm half-max radius), the calculated emittance ($\epsilon=r_o\theta_{hwhm}$) is 0.4 π-mm-mrad. To verify that the reduction in the beam emittance is due to the extension of the plasma channel, another gas jet with a narrower width was used and the same measurements repeated. In this case, the sidescattered images show that the channel length is limited to 360 μm and the electron beam divergence is fixed at 12° for all laser powers.

Waveguide Formation

In order to observe the formation and evolution of the plasma-waveguide structure, probing interferometry and shadowgraphy were used. 3-D images of the plasma-density distribution were obtained in this way at different times. A probe pulse (400 fs, 1.053 μm) is obtained by splitting 5% of the pump pulse, sending it into a delay line, and crossing it perpendicularly with the pump pulse in the interaction region. A lens was used to image the probe pulse in the plasma region to a CCD camera, forming shadowgrams. Inter-
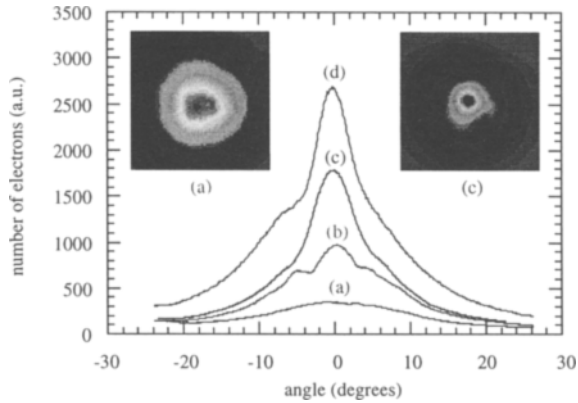

FIGURE 3. Electron beam divergence as a function of laser power. The various curves represent laser powers of $P/P_c =$ (a) 3.4, (b) 5.0, (c) 6.0, and (d) 7.5. The two insert figures show the complete beam images for curves (a) and (c).

ferograms were obtained by use of two glass wedges forming a vacuum wedge gap [23] after the lens. To get quantitative measurements of the evolution of the plasma waveguide, a 3-D plasma density distribution was obtained by means of a fringe tracking program (to get a 2-D phase-shift distribution) in conjunction with an abelization algorithm. Fig. 3 shows the 3D plasma density distribution (cylindrically symmetric) evolving in time. As can be seen, the density depression on axis become deeper and the width of the channel becomes larger as time goes by. At about 40 ps delay, a plasma waveguide of 800 μm in length is formed, which has an on-axis plasma density less than 10^{18} cm^{-3} and a channel width of 30 μm. In Fig. 3, the waveguide length is equal to the self-channeling length of the pump pulse.

REFERENCES

1. P. Maine, D. Strickland, P. Bado, M. Pessot and G. Mourou, *IEEE J. Quantum Electron.* **QE-24**, 398 (1988).
2. G. Mourou and D. Umstadter, *Phys. Fluids B* **4**, 2315 (1992).
3. T. Tajima and J. M. Dawson, *Phys. Rev. Lett.* **43**, 267 (1979).
4. N. E. Andreev, L. M. Gorbunov, V. I. Kirsanov, A. Pogosova and R. R. Ramazashvili, *Pis'ma Zh. Eksp. Teor. Fiz.,* **55** 551 (1992) [*JETP Lett.,* **55**, 571 (1992)].
5. T. M. Antonsen, Jr., and P. Mora, *Phys. Rev. Lett.,* **69**, 2204 (1992).
6. P. Sprangle, E. Esarey, J. Krall, and G. Joyce, *Phys. Rev. Lett.,* **69**, 2200 (1992).
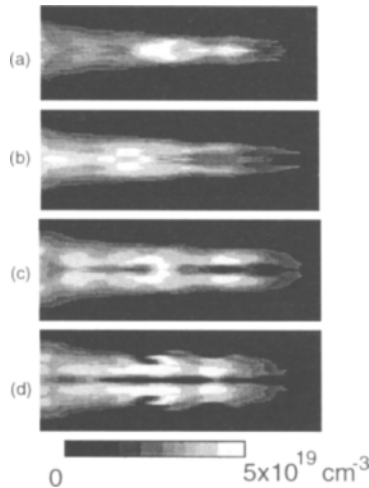
FIGURE 4. 2-D plasma density distribution for 2.5 TW laser power and 2×10^{19} cm^{-3} gas density at different times: (a) 5 ps, (b) 15 ps, (c) 30 ps, and (d) 40 ps.

7. D. Umstadter *et al.*, Science **273**, 472 (1996).

8. M. Tabak *et al.*, Phys. Plasmas **1**, 1626 (1994).

9. E. Esarey *et al.*, IEEE Trans. Plasma Sci. **PS-24**, 252 (1996).

10. G. Z. Sun *et al.*, Phys. Fluids **45**, 526 (1987).

11. A. B. Borisov *et al.*, Phys. Rev. A **45**, 5830 (1992).

12. P. Monot *et al.*, Phys. Rev. Lett. **74**, 2953 (1995).

13. R. Wagner *et al.*, Phys. Rev. Lett. **78**, 3125 (1997).

14. A. Pukhov and J. Meyer-ter-Vehn, Phys. Rev. Lett. **76**, 3975 (1996).

15. D. C. Barnes, T. Kurki-Suonio, T. Tajima, IEEE Trans. Plasma Sci. **PS-15**, 154 (1987).

16. D. Umstadter, S.-Y. Chen, A. Maksimchuk, G. Mourou, and R. Wagner, *Science* **273**, 472 (1996).

17. K. Krushelnick *et al.*, Phys. Rev. Lett. **78**, 2373 (1997).

18. S. P. Le Blanc *et al.*, Phys. Rev. Lett. **77**, 5381 (1996).

19. A. Chiron *et al.*, Phys. Plasmas **3**, 1373 (1996).

20. C. Rousseaux, *et al.*, Phys. Fluids B, **4**, 2589 (1992).

21. K.-C. Tzeng, *et al.*, *Advanced Accelerator Concepts 1996*, to be published.

22. S. Humphries Jr., *Principles of Charged Particle Accelerators* (Wiley, New York, 1986).

23. G. S. Sarkisov, Instruments and Experimental Techniques **39**, 727 (1996).

24. H. Tawara *et al.*, Atomic Data and Nuclear Data Tables **36**, 167 (1987).

25. C. A. Coverdale, C. B. Darrow, C. D. Decker, W. B. Mori, K. -C. Tzeng, K. A. Marsh, C. E. Clayton, and C. Joshi, *Phys. Rev. Lett.* **74**, 4659, (1995).

26. K. Nakajima, D. Fisher, T. Kawakubo, H. Nakanishi, A. Ogata, Y. Kato, Y. Kitagawa, R. Kodama, K. Mima, H. Shiraga, K. Suzuki, K. Yamakawa, T. Zhang, Y. Sakawa, T. Shoji, N. Yugami, M. Downer and T. Tajima, *Phys. Rev. Lett.* **74**, 4428, (1995).

27. A. Modena, Z. Najmudin, A. E. Dangor, C. E. Clayton, K. A. Marsh, C. Joshi, V. Malka, C. B. Darrow, C. Danson, D. Neely and F. N. Walsh, *Letts. Nature* **377**, 606, (1995).

28. A. Ting, K. Krushelnick, C. I. Moore, H. R. Burris, E. Esarey, J. Krall, and P. Sprangle, *Phys. Rev. Lett.* **77**, 5377 (1996).

29. S. P. Le Blanc, M. C. Downer, R. Wagner, S.-Y. Chen, A. Maksimchuk, G. Mourou and D. Umstadter, *Phys. Rev. Lett.* **77**, 5381 (1996).

30. R. Wagner, S.-Y. Chen, A. Maksimchuk and D. Umstadter, *Phys. Rev. Lett.* **78**, 3122 (1997).

31. D. Umstadter, E. Esarey, and J. Kim, Phys. Rev. Lett. **72**, 1224 (1994); D. Umstadter *et al.*, Phys. Rev. E **51**, 3484 (1995).

32. D. Umstadter, J. K. Kim, and E. Dodd, *Phys. Rev. Lett.* **76**, 2073 (1996).

33. E. Esarey and M. Pilloff, Phys. Plasmas **2** 1432 (1995).

34. See *e.g.*, *Advanced Accelerator Concepts, Fontana, WI, 1994*, Amer. Inst. of Conf. Proc. No. 335, P. Schoessow, ed., (AIP Press, New York, 1995) and references cited therein.